

NPS ARCHIVE
1960
FEIT, H.

A HYBRID-SIDEBAND
COMMUNICATIONS SYSTEM

HARRY H. FEIT, JR.

LIBRARY
U.S. NAVAL POSTGRADUATE SCHOOL
MONTEREY, CALIFORNIA

UNITED STATES NAVAL POSTGRADUATE SCHOOL



THESIS

A HYBRID-SIDEBAND
COMMUNICATIONS SYSTEM

by

Harry H. Feit, Jr.

1960

A HYBRID-SIDEBAND
COMMUNICATIONS SYSTEM

Harry H. Feit, Jr.

A HYBRID-SIDEBAND
COMMUNICATIONS SYSTEM

by

Harry H. Feit, Jr.

Lieutenant, United States Navy

Submitted in partial fulfillment of
the requirements for the degree of

MASTER OF SCIENCE
IN
ENGINEERING ELECTRONICS

United States Naval Postgraduate School
Monterey, California

1960

DUDLEY KNOX LIBRARY
NAVAL POSTGRADUATE SCHOOL
MONTEREY CA 93943-5101

A HYBRID-SIDEBAND
COMMUNICATIONS SYSTEM

by

Harry H. Feit, Jr.

This work is accepted as fulfilling
the thesis requirements for the degree of

MASTER OF SCIENCE

IN

ENGINEERING ELECTRONICS

from the

United States Naval Postgraduate School

ABSTRACT

The purpose of this paper is to present a communications system which uses a combination of single and double-sideband techniques. Audio intelligence information is transmitted via single sideband and a single frequency tone is transmitted via double sideband to provide a means of carrier-frequency reinsertion at the receiving terminal. This system provides the power and spectrum conservation achieved by single-sideband techniques, and the means of obtaining the proper frequency for carrier reinsertion at the receiver which can be obtained by synchronous reception of the double-sideband information. The carrier frequency, which is common to both the single and double-sideband signals during the generation process at the transmitter, is suppressed to the fullest possible extent prior to the actual transmission of the sidebands. Use of a narrow bandwidth filter for the double sidebands at the receiver allows the synchronizing tone to be transmitted at a level much lower than that of the intelligence-bearing single sideband, providing economy of transmitted power. The inherent automatic-frequency-control feature of the synchronous detector allows system frequency stability requirements to be lessened, and provides rapid frequency correction to overcome Doppler frequency shifts.

The system presented herein was originally proposed by Professor P. E. Cooper. The writer gratefully acknowledges the guidance and editorial assistance given him by Professor P. E. Cooper and Professor D. B. Hoisington.

TABLE OF CONTENTS

Chapter	Title	Page
I.	Introduction	1
II.	Operation of the Hybrid-Sideband System	7
III.	System Imperfections and Their Associated Effects	28
IV.	The Laboratory Model	35
V.	Conclusions	54
	Bibliography	58
Appendix I	Demodulator Operation When Carrier Component is Present	60
Appendix II	Operation of the Gated Rectifier	62

LIST OF ILLUSTRATIONS

Figure	Page
1. Frequency Spectrum of Hybrid Signal	4
2. Block Diagram of Hybrid-System Demodulator	10
3. Schematic Diagram of Hybrid-System Demodulator	64
4. Frequency Spectrum for Synchronizing Frequency Lower Than Intelligence Frequency	14
5. Frequency Spectrum for Synchronizing Frequency Higher Than Intelligence Frequency	14
6. Frequency Spectrum of Hybrid Signal and Undesired Sideband	15
7. Block Diagram of Phase-Locking Loop	19
8. Block Diagram of Servo Loop	22
9. Basic Lag Network	27
10. Schematic Diagram of Hybrid-System Modulator	65
11. Passband Characteristics of Mechanical Filter	38

CHAPTER I

INTRODUCTION

For many years radio communications involving the transmission and reception of voice information have used the method of amplitude modulation in which the transmitted signal consists of a radio-frequency carrier, and two sidebands which contain the information. The receiving terminal contains a detector which uses the carrier and the sidebands to demodulate this information. Under conditions of maximum modulation the power contained in each sideband is one-quarter of the power transmitted at the carrier frequency. Since the same information is contained in each of the two sidebands, the effective transmitted power which conveys the necessary information is contained in only one sideband and is one-sixth of the total power radiated by the transmitter.

Another means of transmitting voice information is known as single sideband suppressed carrier, or more common as single sideband. This method eliminates the carrier and one of the two sidebands which were used for the conventional amplitude-modulation process. The power eliminated from the carrier and suppressed sideband may be used to increase the power in the one remaining sideband which now conveys the intelligence. Although the carrier which is transmitted in the amplitude-modulation system does not contain any of the voice information, it does provide the receiving demodulator with information concerning its frequency and phase, thus enabling demodulation by simple rectifying methods. With single-sideband transmission this carrier is not present, requiring that the receiver demodulator obtain this phase and frequency information from an oscillator located in the receiver, which is closely synchronized with the frequency determining oscillator in the single-

sideband transmitter. Studies have been made to determine the extent of frequency synchronization required to obtain a demodulator output which permits recovery of the transmitted speech information. Results of these studies are contained in references [10] and [21]. A maximum deviation of about 50 cycles per second has been found to be permissible, requiring that the frequency determining elements of both the transmitter and the receiver be extremely stable if satisfactory communications are to be achieved by the use of single-sideband techniques. If it is desired to communicate with high-speed aircraft, the frequency agreement between the transmitter and the receiver must be better than 50 cycles per second, as the Doppler effect causes an additional frequency shift which can be as much as 90 cycles per second for aircraft speeds of Mach three at frequencies near 30 megacycles per second.

The commercial communications companies and the military services have been using single-sideband methods rather extensively for fixed-station, point-to-point service during the past two decades. The recent availability of more compact, stable frequency determining elements has permitted single-sideband equipments to be constructed for mobile, shipboard, and airborne applications. These frequency determining elements are costly and complex, particularly for military requirements where they must permit operation in large numbers of channels over a very wide range of frequencies.

Another method of voice communications which has gained some popularity during the past few years involves the transmission of a signal identical to that of conventional amplitude modulation except that the carrier frequency is removed. This method is known as double-sideband suppressed carrier, or more commonly, double sideband. Al-

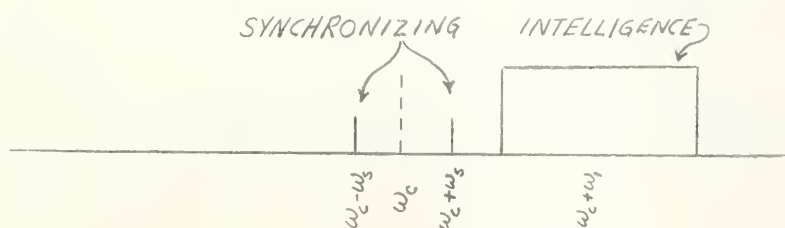
though it requires somewhat more than twice the frequency spectrum of single-sideband transmission, the information regarding the carrier frequency and phase can be derived from these two sidebands by the use of phase-locked synchronous detection techniques, as shown by Costas [4]. The accuracy of synchronism between the transmitter and receiver frequency determining elements as required for single-sideband usage can be lessened when double-sideband transmission is employed, as the synchronous detector can provide much of the required frequency and phase information.

The purpose of this paper is to present a hybrid-sideband communications system which utilizes a combination of both the double and single-sideband techniques in order to achieve the power and spectrum conservation features of single sideband, and the frequency and phase information transmission feature of double sideband. This system transmits the voice (intelligence) information in a single sideband, and a single-frequency tone on double sidebands for receiver synchronizing. The additional frequency spectrum required for this hybrid method is only 550 cycles per second greater than that required for pure single-sideband transmission. Power in each of the two sidebands used for synchronizing can be reduced to a level 30 decibels less than that contained in the intelligence-bearing single sideband, so that the additional power required to achieve the automatic synchronizing feature is comparatively small.

The configuration of the circuitry required for the phase-locked synchronous detector permits simultaneous single-sideband reception to be obtained by the phasing method described by Norgaard [1] with only a relatively few additional components required. This feature, in con-

junction with the reduced frequency stability required with the hybrid sideband system, should allow more economical construction of the transmitters and receivers than is possible for comparable single-sideband equipments. Also, the inherent automatic-frequency-control feature of the phase-locked synchronous detector will provide rapid correction for frequency shifts caused by Doppler effect.

Figure 1 shows the output spectrum of the hybrid sideband system modulator when the audio frequency synchronizing tone is of lower frequency than the frequencies which contain the intelligence information.



FREQUENCY SPECTRUM OF HYBRID SIGNAL

FIGURE 1

Normally, the carrier frequency employed in the modulator will be on the order of hundreds-of-kilocycles per second, as sideband filtering can be most easily accomplished in this frequency range. The output frequency of the basic modulator is translated to the actual radiating frequency by means of mixer circuitry. The mixer and all succeeding amplifier stages must necessarily be capable of linear operation in order to faithfully transmit the modulated signal.

The modulator portion of the hybrid sideband system must perform the following functions:

- A. Accept the intelligence information in the form of an audio-frequency voltage.
- B. Generate the radio-frequency carrier signal.

- C. Modulate the radio-frequency carrier with the intelligence information.
- D. Remove the carrier-frequency component from the modulated signal.
- E. Remove one of the two sidebands which were generated during the modulation process.
- F. Generate a single audio-frequency signal.
- G. Modulate the radio-frequency carrier with the single audio-frequency signal.
- H. Remove the carrier-frequency component from this modulated signal.
- I. Combine the resultant signals which were obtained in (E) and (H) above.

The demodulator portion of the hybrid sideband system must perform the following functions:

- A. Accept the received signal of the form shown in Figure 1.
- B. Obtain information regarding the frequency and phase of the carrier from the double-sideband components of the received signal, and use this information to provide a reinjection carrier of the proper frequency and phase. This phase information is not required for reception of voice information, however, this feature is inherent in the synchronous detector and will be required if binary data reception should be desired.
- C. Suppress the single-tone audio frequency which was used for step (B) in order that it will not be combined with the recovered intelligence information.
- D. Provide a means to achieve the minimum spectral bandwidth re-

quired for the demodulation of the intelligence information.

- E. Provide a means for accepting intelligence which is selectively transmitted in either the upper or lower sideband position, while maintaining the minimum bandwidth requirements.
- F. Amplify and transform impedances to enable the intelligence information to be accurately reproduced by an audio transducer.
- G. Provide sufficient frequency selectivity in the circuitry associated with the carrier synchronizing to permit the single frequency audio tone to be transmitted at a minimum power level.
- H. Provide an automatic-gain-control feature to allow optimum operation of the demodulator under conditions of wide variations of the intensity of the received signal.

CHAPTER II

OPERATION OF THE HYBRID SIDEBAND SYSTEM

The transmitted signal is of the form shown in Figure 1. The method used to generate this type of hybrid signal will be completely described in a subsequent section of this paper.

The two single-frequency sidebands which are equally spaced about the reference carrier frequency, ω_c , represent the output of a balanced modulator, or similar device, and are of the form:

$$(1) \quad e_s = \frac{mE_c}{2} \left[\cos(\omega_c - \omega_s)t + \cos(\omega_c + \omega_s)t \right]$$

The designation, e_s , is used to represent that portion of the hybrid signal used for synchronizing purposes.

The single-sideband portion of the hybrid signal shown in Figure 1 represents the intelligence-bearing component and can be described as shown below. For purposes of this treatment the transmitted information will be considered as a single frequency, since the actual intelligence to be transmitted can be represented as a series of single frequencies as determined by its Fourier components.

$$(2) \quad e_i = ME_c \cos(\omega_c + \omega_s)t$$

The hybrid signal as transmitted is comprised of both the synchronizing information designated as e_s , and the intelligence information designated as e_i , and is of the form:

$$(3) \quad e_t = \frac{mE_c}{2} \left[\cos(\omega_c - \omega_s)t + \cos(\omega_c + \omega_s)t \right] + ME_c \cos(\omega_c + \omega_s)t$$

Where e_t represents the transmitted signal used with the hybrid communications system.

A block diagram of the demodulator is shown in Figure 2. The input to this demodulator circuitry can be either at the transmitted or at an intermediate frequency. Both of these possible usages will be described in a latter portion of this chapter, however, operation at the radio carrier (transmitted) frequency will be assumed for this analysis. It will be shown that identical results are obtained for intermediate-frequency employment if the radio-frequency portion of the receiver circuitry is capable of linear amplification without non-linear phase shifts throughout the passband required for the hybrid signal.

SIGNAL PATH ANALYSIS

Reference should be made to Figure 2 for the following signal path analysis.

The received hybrid signal, e_t , is applied to the inputs of a pair of identical product detectors. A reinserted carrier is also applied to these detectors through a phase shifting network. The detector shown as "I Channel" receives this carrier in phase synchronism with the carrier, ω_c , which was used for the generation of the hybrid signal in the modulator portion of the transmitter. The detector shown as "Q Channel" receives the reinserted carrier after it has been phase-shifted by ninety degrees from that applied to the I channel detector. These two reinserted carriers are represented as:

$$(4) \quad e_{c_i} = A \cos \omega_c t$$

$$(5) \quad e_{c_q} = B \sin \omega_c t$$

The method used to obtain this phase synchronized reinsertion carrier will be described in a later section of this chapter.

The I channel product detector receives the two signals:

$$(6) \quad s = A \cos(\omega_c t) + m \cos(\omega_s t)$$

$$(7) \quad e_{ci} = A \cos \omega_c t$$

Norgaard [1], has shown that the output of a product detector may be expressed as the mathematical product of the two input signals. The output of this I channel product detector is:

$$(8) \quad e_{ci} = e_c \times e_{ci} \\ = \frac{1}{2} \left[\frac{mAE_c}{2} \cos(\omega_c + \omega_s + \omega_c)t + \frac{mAE_c}{2} \cos(\omega_c + \omega_s - \omega_c)t \right. \\ \left. + MAE_c \cos(\omega_c + \omega_c + \omega_s)t + MAE_c \cos(\omega_c + \omega_c - \omega_s)t \right. \\ \left. + \frac{mAE_c}{2} \cos(\omega_c - \omega_s + \omega_c)t + \frac{mAE_c}{2} \cos(\omega_c - \omega_s - \omega_c)t \right]$$

which simplifies to:

$$(9) \quad e_{ci} = \frac{AE_c}{2} \left[\frac{m}{2} \cos(2\omega_c + \omega_s)t + m \cos \omega_s t + \frac{m}{2} \cos(2\omega_c - \omega_s)t \right. \\ \left. + M \cos(2\omega_c + \omega_s)t + M \cos \omega_s t \right]$$

The Q channel product detector receives the two signals:

$$(10) \quad e_c = \frac{mE_c}{2} \left[\cos(\omega_c + \omega_s)t + \cos(\omega_c - \omega_s)t \right]$$

$$(11) \quad e_{cq} = B \sin \omega_c t$$

Output from this detector is:

$$(12) \quad e_{oq} = e_c \times e_{cq}$$

Using the trigonometric relationship:

$$(13) \quad \sin x \cos y = \frac{1}{2} \left[\sin(x+y) + \sin(x-y) \right]$$

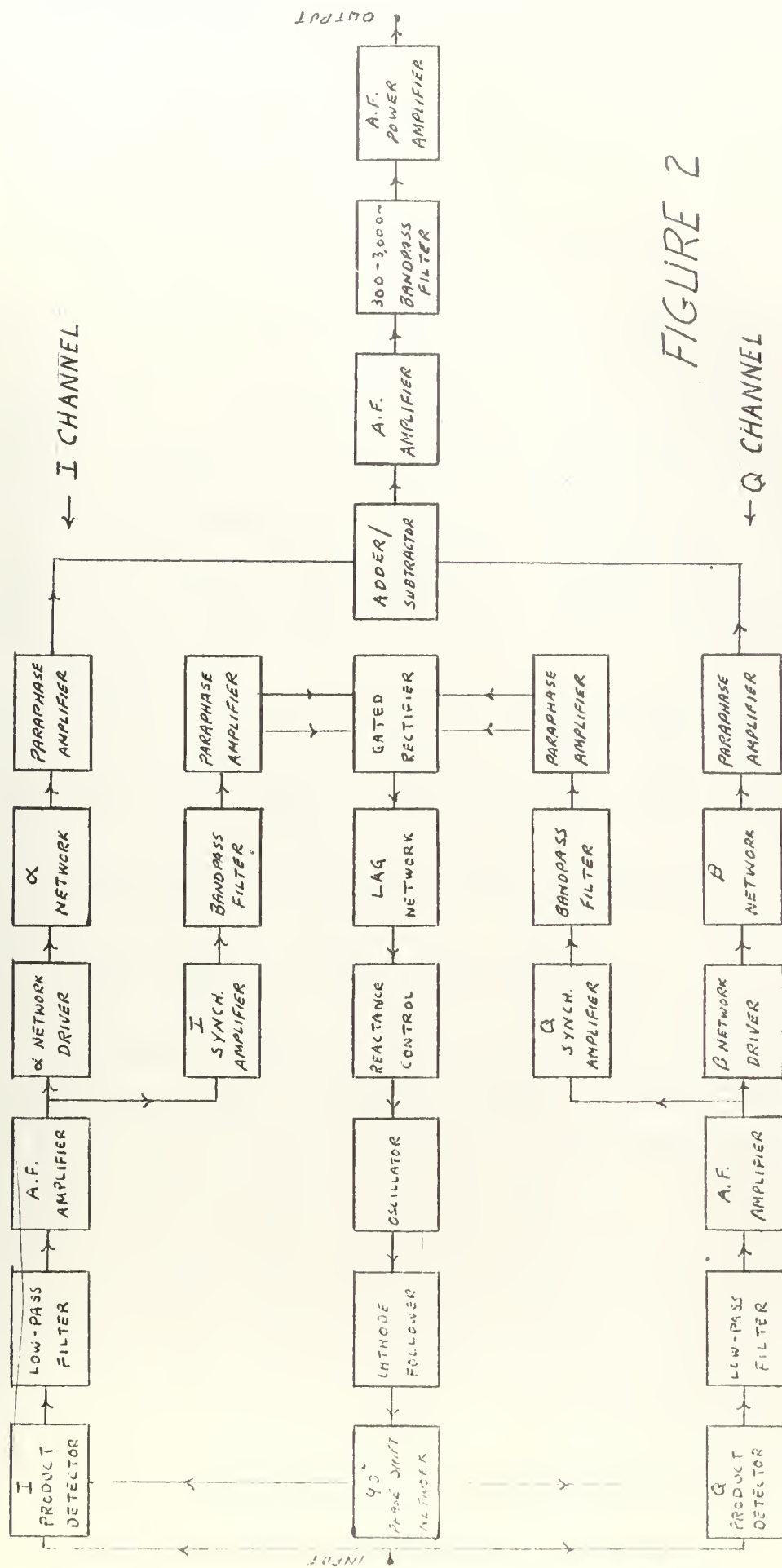


FIGURE 2

BLOCK DIAGRAM-HYBRID SYSTEM DEMODULATOR

$$e_{sq} = \frac{1}{2} B E_c \left[\cos(\omega_s t + \omega_c + \omega_1) + \cos(\omega_s t + \omega_c - \omega_1) + \sin(\omega_c - \omega_s + \omega_1) t \right. \\ (14) \quad \left. + \sin(\omega_c - \omega_s - \omega_1) t \right] + \frac{1}{2} M E_c \left[\sin(\omega_s t + \omega_c + \omega_1) + \sin(\omega_s t + \omega_c - \omega_1) \right]$$

Which simplifies to:

$$(15) \quad e_{sq} = \frac{B E_c}{2} \left[\frac{m}{2} \sin(2\omega_s + \omega_1) t - \frac{m}{2} \sin \omega_1 t + \frac{M}{2} \sin(2\omega_s - \omega_1) t \right. \\ \left. + \frac{M}{2} \sin \omega_1 t + M \sin(2\omega_s + \omega_1) t - M \sin \omega_1 t \right]$$

A low-pass filter with a cutoff frequency greater than ω_1 , but less than ω_c is placed at the output of each of the product detectors. Figure 2 indicates this filter placement. The amplitude and phase characteristics of these filters must be nearly identical in order that the I and Q channels will be symmetrical. Ideal filters are assumed for this analysis. The effects of non-ideal characteristics will be treated in Chapter 3.

At the output of the I channel low-pass filter:

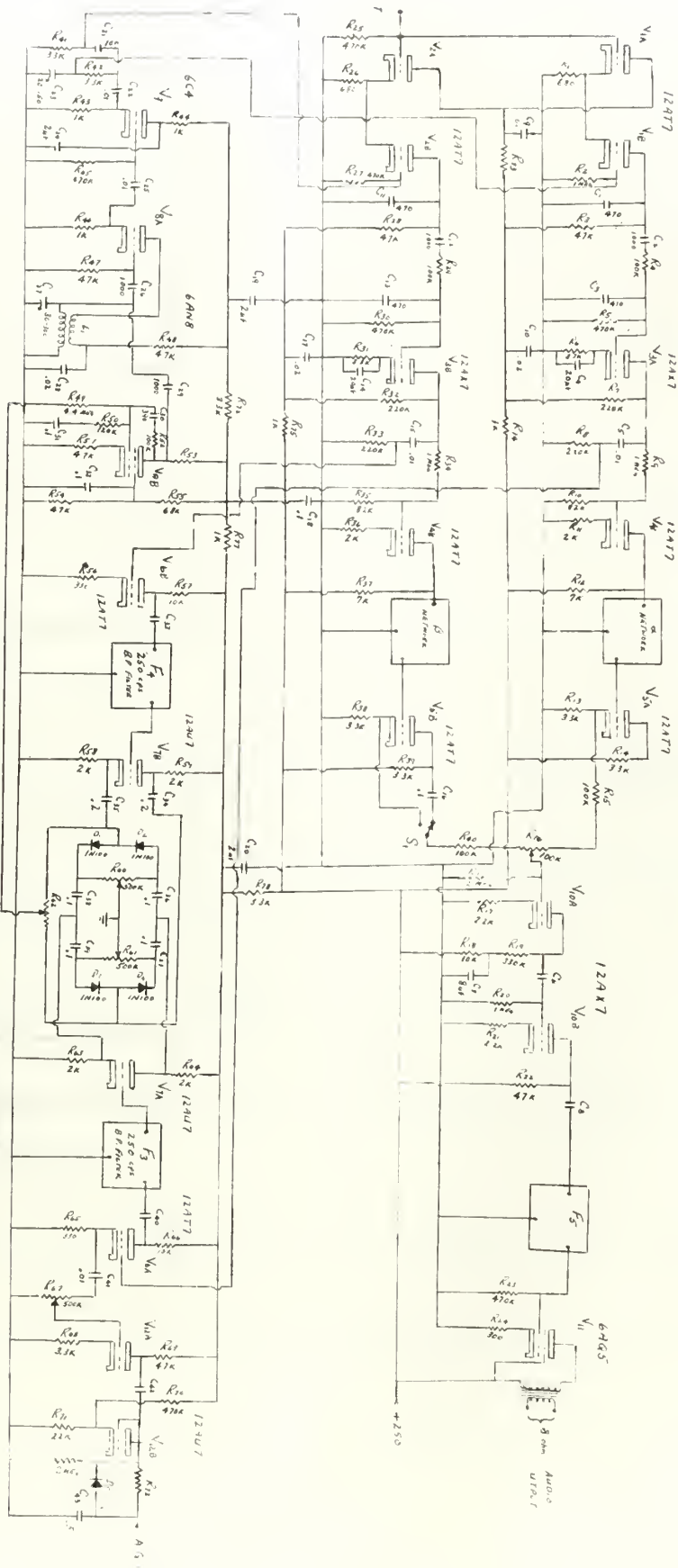
$$(16) \quad e_{si} = \frac{A E_c}{2} \left[m \cos \omega_s t + M \cos \omega_1 t \right]$$

The output of the Q channel low-pass filter is:

$$(17) \quad e_{sq} = - \frac{B M E_c}{2} \sin \omega_1 t$$

Inspection of Equation (17) reveals that the output of the Q channel low-pass filter contains no component of the synchronizing signal, ω_s , when the reinserted carrier is in phase synchronism with the carrier used to generate the hybrid signal.

The outputs from the low-pass filters are fed to the phase-locking circuitry and to the phase-shifting networks as can be seen from Figure 3. These phase-shifting networks must have characteristics which remain substantially constant throughout the frequency spectrum required for the hybrid signal. If practical considerations should cause difficulties



HYBRID SIDEBAND DEMODULATOR

in achieving a ninety-degree phase shift at the lower audio frequency of ω_s , band rejection filters tuned to remove this frequency could be inserted prior to the phase-shifting networks. This should be avoided when possible as the practical difficulties encountered in maintaining identical phase and amplitude characteristics in the two channels become greatly magnified as additional filters are included.

The characteristics of the phase-shifting networks are:

$$(18) \quad \alpha = \beta + 90^\circ$$

where α and β are the phase-shifting angles of the networks installed in the I and Q channels, respectively.

The input to the α network (I Channel) is e_{fi} as given in Equation (16). Output of this network is:

$$(19) \quad e_\alpha = \frac{AE_c}{2} \left[m \cos(\omega_s t + \alpha) + M \cos(\omega_i t + \alpha) \right]$$

Input to the β network (Q Channel) is e_{fq} , as given by Equation (17). Output of this network is:

$$(20) \quad e_\beta = -\frac{BME_c}{2} \sin(\omega_i t + \beta)$$

Rewriting Equation (19) to include the relationship given by Equation (18):

$$(21) \quad e_\alpha = \frac{AE_c}{2} \left[m \cos(\omega_s t + \beta + 90^\circ) + M \cos(\omega_i t + \beta + 90^\circ) \right]$$

Using the trigonometric relationship: $\cos(\chi + 90^\circ) = -\sin \chi$

$$(22) \quad e_\alpha = \frac{AE_c}{2} \left[-m \sin(\omega_s t + \beta) - M \sin(\omega_i t + \beta) \right]$$

The outputs from the α and β networks are fed to an electrical

adding network which provides the mathematical sum of the e_1 and e_2 voltages described by Equations (22) and (20).

$$(23) \quad e_1 + e_2 = -\left[\frac{AE}{2} \sin(\omega_c t + \mu) + \frac{AE}{2} \sin(\omega_c t - \mu) + \frac{BNE}{2} \sin(\omega_c t + \beta) \right]$$

When the two quadrature outputs from the carrier-reinsertion phase-shifting network have equal amplitudes, the coefficients A and B are identical. Under this condition the output of the additive network is:

$$(24) \quad e_{out} = -AE_c \left[M \sin(\omega_c t + \mu) + \frac{N}{2} \sin(\omega_c t + \beta) \right]$$

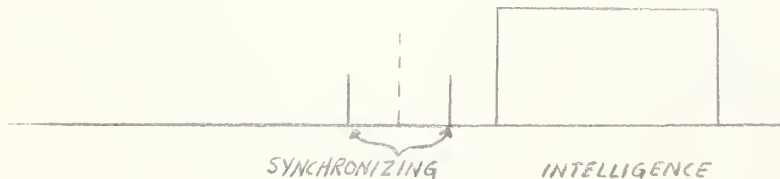
This signal is then passed through a band-pass filter which removes the component of the synchronizing frequency, ω_c , while passing that portion of the frequency spectrum which contains the intelligence information. The output of the demodulator consists of only the modulated intelligence information which has been phase shifted by an amount β . The angle β is arbitrary and constant throughout the frequency spectrum required for the intelligence information, so that it has no effect upon the demodulated information output.

Theoretically the α and β networks are not both required since they only serve to provide a ninety degree phase difference between the I and Q channel signals. This function could be accomplished by placing a single ninety degree phase shift network in the I channel. Norgaard [10], Dome [2], and Darlington [3], have shown that practical difficulties preclude the reality of a network which provides a constant ninety degree phase shift over a wide frequency range. The authors have shown that the use of constant phase difference networks provides optimum results with the techniques in use at the present time.

Such networks are commercially available

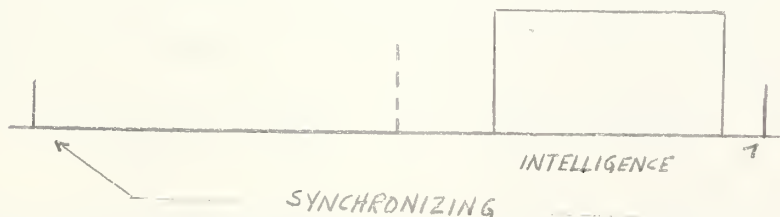
SELECTION OF A SYNCHRONIZING FREQUENCY

The preceding example was based upon the use of a synchronizing frequency which was lower than the range of frequencies used to convey the intelligence information. The synchronizing frequency could be located above the frequency spectrum required for the intelligence, however, such positioning would necessarily increase the spectrum width required for transmission of the hybrid signal. The effects of such positioning are shown in Figures 4 and 5.



SYNCHRONIZING FREQUENCY LOWER THAN INTELLIGENCE FREQUENCIES

Figure 4



SYNCHRONIZING FREQUENCY HIGHER THAN INTELLIGENCE FREQUENCIES

Figure 5

SINGLE-SIDEBAND SELECTIVITY

A portion of the demodulator required for the hybrid sideband system, as shown in Figure 2, is quite similar to that given by Norgaard [1] for obtaining single-sideband selectivity by the phasing technique. Norgaards' system was intended only for reception of single-sideband signals, however, the inclusion of the carrier reinsertion-

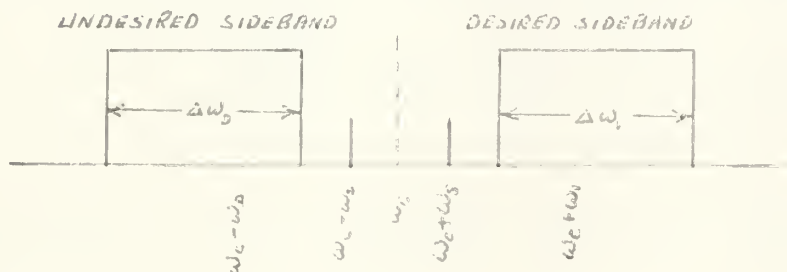
oscillator phase-locking circuitry as shown by Costas [4] and Webb [5] provide the basis for the hybrid-sideband system.

The following example serves to illustrate the single-sideband selectivity characteristics of the detector that is used for the hybrid system:

Assumptions:

- (1) Double-sideband synchronizing frequency is lower than frequencies used to convey intelligence.
- (2) Intelligence information is contained in the upper sideband, and is represented as $(\omega_c + \omega_s)$.
- (3) Interfering signal is present in the lower sideband, has a bandwidth $\Delta\omega_d$ and is not phase-related to the carrier frequency signal, .
- (4) Reinsertion oscillator is phase locked to the carrier signal used to generate the signal at the hybrid system modulator.

Figure 6, shown below, illustrates the occupancy of the frequency spectrum in the vicinity of the transmitted hybrid system signal



HYBRID SIGNAL WITH LOWER SIDE BAND INTERFERENCE

FIGURE 6

This composite signal is comprised of both desired and undesired components, and is represented as:

$$(25) \quad e_s = A \cos \omega_c t + B \cos \omega_s t + C \sin \omega_c t + D \sin \omega_s t$$

The I channel product detector receives both e_s and the in-phase reinserted oscillator signal, $D \cos \omega_c t$. The output of this detector is:

$$(26) \quad \begin{aligned} e_{oi} &= e_s \times D \cos \omega_c t \\ &= \frac{AD}{2} [\cos(2\omega_c - \omega_c)t + \cos(\omega_c + \omega_c)t] + \frac{BD}{2} [\cos(2\omega_c - \omega_s)t \\ &\quad + \cos(\omega_c + \omega_s)t + \cos \omega_c t] \\ &\quad + \frac{CD}{2} [\cos(2\omega_c + \omega_c)t + \cos \omega_c t] \end{aligned}$$

The Q channel product detector receives both e_s and the phase shifted reinsertion oscillator signal, $D \sin \omega_c t$. The output of this detector is:

$$(27) \quad \begin{aligned} e_{oq} &= e_s \times D \sin \omega_c t \\ &= \frac{AD}{2} [\sin(2\omega_c - \omega_c)t + \sin \omega_s t] + \frac{BD}{2} [\sin(2\omega_c - \omega_s)t \\ &\quad + \sin \omega_s t + \sin(2\omega_c + \omega_s)t + \sin(-\omega_s)t] \\ &\quad + \frac{CD}{2} [\sin(2\omega_c + \omega_c)t + \sin(-\omega_c)t] \end{aligned}$$

After passing through the low-pass filters which follow the product detectors, the outputs will be:

$$(28) \quad e_{fi} = \frac{AD}{2} \cos \omega_b t + BD \cos \omega_s t + \frac{CD}{2} \cos \omega_c t$$

$$(29) \quad e_{fq} = \frac{AD}{2} \sin \omega_b t - \frac{CD}{2} \sin \omega_c t$$

These two signals are then passed through the wideband phase-shift networks which were described in an earlier portion of this chapter. The I channel network inserts a phase shift of β degrees, the Q channel network a phase shift of $\beta + 90$ degrees, where β is the phase shift of the reference carrier. At the output of these networks:

$$(30) \quad e_{i1} = \frac{A_D}{2} \cos(\omega_c t + \beta) \cos(\omega_i t + \theta) + \frac{A_D}{2} \cos(\omega_c t + \beta) \sin(\omega_i t + \theta)$$

$$(31) \quad e_{q1} = \frac{A_D}{2} \sin(\omega_c t + \beta) \cos(\omega_i t + \theta) - \frac{A_D}{2} \sin(\omega_c t + \beta) \sin(\omega_i t + \theta)$$

and since: $\cos(\alpha + 90) = -\sin \alpha$

$$(32) \quad e_{q1} = -\frac{A_D}{2} \sin(\omega_c t + \beta) \cos(\omega_i t + \theta) - \frac{A_D}{2} \sin(\omega_c t + \beta) \sin(\omega_i t + \theta)$$

These signals are then applied to the electrical addition network. the output of this network is:

$$(33) \quad e_{out} = - \left[C D \sin(\omega_i t + \theta) + B D \sin(\omega_i t + \theta) \right]$$

After passing through a filter which removes the ω_c component, the intelligence output shown below is obtained:

$$(34) \quad e_f = - C D \sin(\omega_i t + \theta)$$

As shown earlier in the chapter, the negative sign and phase shift of β degrees do not effect the recovery of the intelligence information.

It can be seen from the above analysis that interference which occurs on the opposite side of the reference-carrier frequency from the placement of the intelligence information will be removed. In practice this interference will not be completely removed, but can be greatly suppressed. This imperfection is a result of channel unbalance and imperfect phase

shifting, and will be treated in greater detail in the subsequent chapter.

If the desired intelligence information is transmitted in the lower sideband, interference which occurs in the upper sideband will be rejected. This may be seen if the notation $(\omega_c - \omega_m)$ is considered as representing the desired sideband, and $(\omega_c + \omega_m)$ as representing the interfering signal. A subtractive rather than an additive network is required in the demodulator, and would provide the mathematical difference of the quantities given by Equations (31) and (32). The resulting filtered output will be:

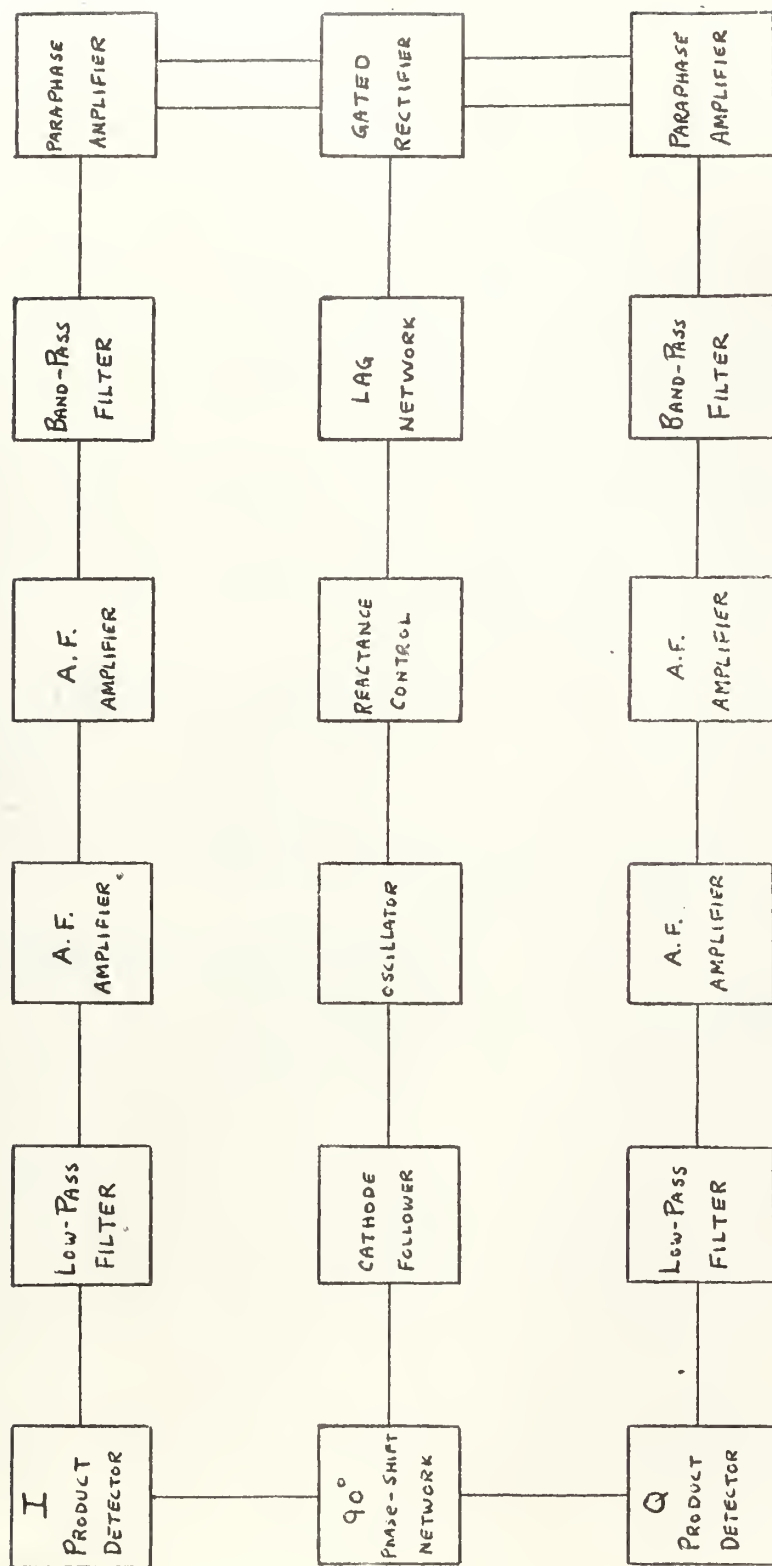
$$(35) \quad e_f = AD \sin(\omega_m t + \phi)$$

The gated rectifier, filter, and reactance control circuitry shown in Figure 7 are used to provide the phase locking of the carrier-reinsertion oscillator. Operation of this circuitry may be shown by considering the signal input to the demodulator to consist of only the double-sideband synchronizing frequency. This is permissible since the band-pass filters between the outputs of the I and Q channel product detectors and the gated rectifier will pass only a narrow band of frequencies centered about that of the synchronizing tone.

The synchronizing portion of the hybrid input signal to the demodulator is represented as:

$$(36) \quad e_m = E \cos(\omega_c - \omega_s)t + E \cos(\omega_c + \omega_s)t$$

This signal and $C \cos(\omega_c t + \phi)$ are applied to the I channel product detector. If the phase difference between the reinserted oscillator signal, and the carrier-frequency signal used to generate the



PHASE-LOCKING LOOP

FIGURE 7

hybrid signal is represented by ϕ , the output of this detector is:

$$(37) \quad e_t = \frac{EC}{2} [\cos(\omega_c t + \phi) + \cos(\omega_c t - \phi)]$$

After passing through the filters:

$$(38) \quad e_{t1} = \frac{EC}{2} \cos(\omega_c t + \phi) + \frac{EC}{2} \cos(\omega_c t - \phi)$$

The input to the Q channel product detector consists of e_t as given by Equation (6), and $C \sin(\omega_s t + \phi)$. The output of this detector is:

$$(39) \quad \begin{aligned} e_{c2} &= e_{t1} \times C \sin(\omega_s t + \phi) \\ &= \frac{EC}{2} [\sin(2\omega_c t - \omega_s t + \phi) + \sin(\omega_s t + \phi) \\ &\quad + \sin(2\omega_c t + \omega_s t + \phi) + \sin(\phi - \omega_s t)] \end{aligned}$$

which after filtering becomes:

$$(40) \quad e_{f2} = \frac{EC}{2} [\sin(\omega_s t + \phi) + \sin(\phi - \omega_s t)]$$

Equations (38) and (40) may be rewritten as shown below by invoking the following trigonometric relationships:

$$(41) \quad \cos(x+y) = \cos x \cos y - \sin x \sin y$$

$$(42) \quad \cos(x-y) = \cos x \cos y + \sin x \sin y$$

$$(43) \quad \sin(x+y) = \sin x \cos y + \cos x \sin y$$

$$(44) \quad \sin(x-y) = \sin x \cos y - \cos x \sin y$$

$$(45) \quad e_{t1} = EC [\cos \omega_c t] [\cos \phi]$$

$$(46) \quad e_{f2} = EC [\cos \omega_s t] [\sin \phi]$$

Examination of these two equations reveals that the inputs to the gated rectifier from the I and Q channel product detectors are identical except for the ninety-degree phase difference of the phase error, ϕ .

Weaver [6], and Wood and Whyland [9], have shown that the gated rectifier performs in a manner similar to a product multiplier which has the additional property of removing the audio-frequency components and only passing the direct-current component. The output of the gated rectifier becomes:

(47)

$$e_{\phi} = \frac{1}{2} (E_c - E_c \cos 2\phi) \sin \phi$$

Due to the inherent elimination of the audio frequency component this becomes:

(48)

$$e_{\phi} = \left(\frac{E_c}{2} \right) \sin \phi$$

This equation represents the phase-control voltage obtained from the gated rectifier. A qualitative analysis of the operation of this circuit by Nupp [7], reproduced as Appendix II, illustrates the actions described above.

McAleer [8] has shown that an entire phase-control loop may be analyzed by the use of servomechanism analogs. The phase-control loop of the hybrid-system demodulator is shown in Figure 8. G_1 represents the transfer function of the phase detector and possesses the units of volts-per-radian. G_2 represents the combined transfer function of the variable reactance and the controlled oscillator. The dimensions of this function are radians-per-second-per volt. The low-pass filter situated between the phase detector and the variable reactance has a

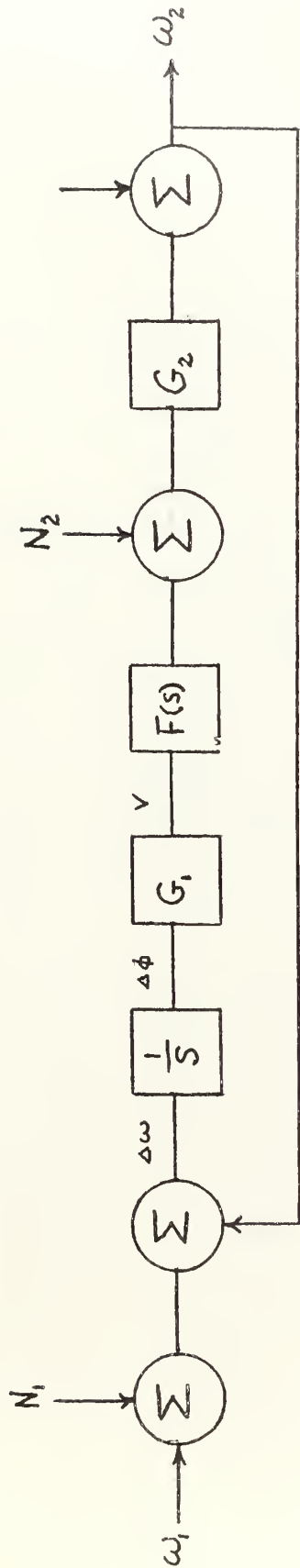


FIGURE 8

SERVO BLOCK DIAGRAM

transfer function designated as $P(s)$. N_1 represents the noise input to the phase-locking system from the inputs to the gated rectifier, and N_2 signifies the noise voltage presented to the input of the variable reactance.

The three most important parameters of the phase-locking system are:

- (a) Lock range
- (b) Capture range
- (c) Filter bandwidth

Lock range is defined as the total frequency drift which can be corrected by the phase-locking system. If the variable reactance is assumed to possess a linear transfer characteristic, the lock range will be $G_1 G_2$ radians per second.

Capture range is defined as the greatest frequency difference for which the system can become locked from its unlocked state. As will be shown subsequently, this range will necessarily be equal to or less than the lock range.

The filter bandwidth of the phase-locking system is indicative of the ability of the system to function properly in the presence of wide-band noise. The injection of the noise, N_1 , into the phase-locking system from the product detectors is external to the internally-closed feedback loop causing the system to appear as a low-pass filter with respect to this noise. The internal system noise, N_2 , is coupled directly to the variable reactance, and indirectly through the feedback path, causing the system to appear as a high-pass filter for noise from this source.

The primary purpose to be served by this loop is the correction of

slow drift of the frequencies in the entire hybrid sideband system. An extremely narrow loop-bandwidth would appear to be optimum for this service since the signal-to-noise figure of the synchronizing circuitry could be maximized. Unfortunately this cannot be realized as the capture range and lock range are reduced as the bandwidth of the phase loop is reduced.

Craiglow and Marlin [10], have indicated that single-sideband frequency inaccuracies in excess of 50 cycles per second are not tolerable for reliable communications. In order to utilize the phase-locking feature of the hybrid system for practical communications purposes the lock range must be a minimum of 200 cycles per second. This would provide automatic frequency compensation for system frequency errors and Doppler shift of plus and minus 150 cycles per second, allowing the use of frequency generating devices with tolerances of three hundred percent less than those required for conventional single-sideband employment.

To effect economy of transmitted power it is most desirable to minimize the power required for the synchronizing tones. The balancing action of the gated rectifier provides excellent isolation of the thermal and impulse noise from the phase-control loop. Additional isolation is provided by the bandpass filters whose pass bands are centered about the synchronizing tone frequency. Laboratory measurements of this ability will be described in Chapter IV.

If a lock range of 300 cycles per second were used, the total noise-bandwidth of the phase-locking loop would be three hundred cycles per second, whereas the noise bandwidth of the information channel would be approximately 3,000 cycles per second. If the same signal-to-noise ratio was required for both the synchronizing and intelligence channels,

the average transmitted power required for the synchronizing tones would be one-tenth of that required for the intelligence information based upon a ten-to-one ratio of noise bandwidths.

Gruen [11], has shown that the use of a lag network for the low-pass filter in the phase-control loop provides optimum reduction of the overall loop bandwidth while retaining the widest possible capture and lock ranges. Insertion of this filter configuration produces a reduction in the capture range that is approximately equal to the square root of the phase-lock-system bandwidth reduction. Simpler resistance-capacitance configurations reduce the capture and lock range in direct proportion to the bandwidth reduction.

A schematic representation of the basic lag network is shown in Figure 9. The transfer function of this network is:

$$(49) \quad T(s) = \frac{1}{1 + s t_1 + s^2 t_2}$$

$$\text{where: } t_1 = \frac{R_1 C_1}{1 + R_1 C_1 s} \quad \text{and } t_2 = \frac{R_1 R_2 C_1 C_2}{1 + R_1 C_1 s}$$

The block diagram of the phase-locking loop as shown in Figure 7 indicates bandpass filters in each of the two inputs to the gated rectifier, as discussed previously. In order that the input impedance characteristics of these low-frequency bandpass filters do not cause serious phase shifts to the higher-frequency components of the intelligence information, it is considered desirable to place isolating amplifiers between the bandpass filters and the outputs of the low-pass filters which succeed the product detectors. The gain characteristics of these amplifiers must be included in the transfer function represented as G_1 . Effects of phase shifts within the passband of the bandpass filter are minimized by design considerations.

The overall transfer function of the phase-locking system is given by McAleer [8] as:

(50)

the denominator being of the form:

(51) Where:

(52)

(53)

With the lag network as shown in Figure 9 used as the low pass filter between the gated rectifier and the variable reactance the capture and lock ranges are shown by Gruen [11] to be:

(54)

(55)

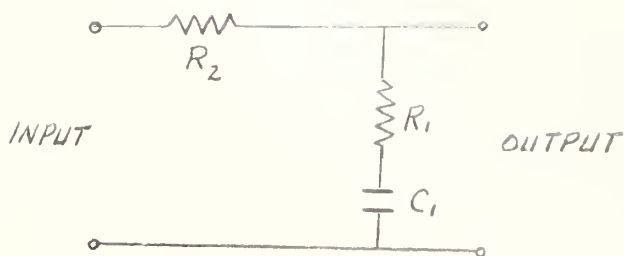
When a damping factor, ζ , of one-half is used to obtain optimum overshoot and lock stabilization:

(56)

(57)

From Equation () the value of t_1 may be found:

(58)



LAG NETWORK

FIGURE 9

The values of lock and capture range which are obtained with actual circuitry can be expected to vary appreciably from those determined by Equations (56) and (57). This difference is caused by the variation of sensitivity of the variable reactance circuitry which is a function of applied bias, and a gated rectifier whose output is not linearly proportional to the phase difference of the input signals. It will be shown in Chapter IV that such a variance was obtained.

CHAPTER III

SYSTEM IMPERFECTIONS AND THEIR EFFECTS

There are six major imperfections which may appear in a practical system of the type described:

- (1) Non-uniform phase shift in the phase-difference networks used to achieve suppression of the undesired sideband.
- (2) Lack of amplitude symmetry in the I and Q demodulator channels.
- (3) Intermodulation distortion and non-uniform phase characteristics of the radio amplifiers which precede the hybrid-system demodulator.
- (4) Carrier-frequency leakage in the modulator.
- (5) Intermodulation distortion in the mixer and amplifier stages of the transmitter.
- (6) Improper demodulator operation due to wide variations of the amplitude of the received signal.

The problems involved in obtaining ninety-degree-phase-difference networks have been thoroughly discussed by Laden [12] and Norgaard [13]. The basic networks in common use today are based upon an original design by Dome [2]. Detailed studies by Laden [12] have shown that variations of five degrees from the optimum value of ninety degrees occur for frequencies between 250 and 3000 cycles per second. Villard [14] and Darlington [3] have proposed more elaborate networks which have superior properties, however the complexities provide many practical problems. Discussion with persons experienced in the manufacture and testing of these more complex networks indicates that tolerances of less than one degree of phase-shift variation cannot be practically achieved at the

present state of the art.

Norgaard [1], has treated the effects of non-perfect phase-difference networks upon the operation of the type demodulator used for the hybrid system. His conclusions indicate that:

$$(59) \quad \frac{\text{Rejected sideband response}}{\text{Accepted sideband response}} = \tan^2 \frac{\theta}{2}$$

where: θ represents the realized phase difference from ninety degrees.

The problems which arise due to a difference in the amplitude characteristics of the I and Q channels are identical to those caused by unequal amplitudes of the two reinserted-oscillator voltages. This effect is apparent by inspection of Equations (20) and (22), where the coefficients A and B represent the oscillator amplitudes. If these coefficients are non-identical, the intelligence output from the demodulator will not be that represented by Equation (24), but will become:

$$(60) \quad e_{out} = -EC \left[\frac{A+B}{2} \sin(\omega_c t + \theta) + (A-B)N \sin(\omega_c t + \theta) \right]$$

causing the amplitude of the intelligence output to be reduced by the difference between the amplitude gains of the two channels.

Icenbice and Felhauer [16] show the intermodulation products resulting from non-linearities to be of the form $(2f_1 - f_2)$ and $(2f_2 - f_1)$. These are normally the most troublesome of the many products formed since it is possible for them to produce relatively high-amplitude signals within the desired passband. To illustrate the effects of this type of undesirable operation, consider the three basic frequencies which comprise the hybrid sideband system signal, as shown in Figure (1). These

components are:

$$(61) \quad (a)$$

$$(b)$$

$$(c)$$

$$(62) \quad 2a-b =$$

$$(63) \quad 2b-a =$$

$$(64) \quad 2c-b =$$

$$(65) \quad 2b-c =$$

$$(66) \quad 2c-a =$$

$$(67) \quad 2a-c =$$

Examination of Equations (62) through (67) shows that two of the third order products will cause interfering components to be generated within the intelligence passband, $\Delta\omega$, when the synchronizing frequency is chosen to be lower than this passband. If the synchronizing frequency is higher than the intelligence passband, the product generated by the combination shown in Equation (65) will cause undesired outputs to lie within the frequency spectrum of the intelligence information. Such effects would cause the desired information to be unfaithfully reproduced.

TRANSMITTER NON-LINEARITIES

Non-linearities which may exist in the mixing and amplifying stages of the transmitter will also cause intermodulation products to be generated. The effects of these products upon the action of the demodulator are identical to those discussed in the preceeding section.

Equations (62) through (67) represent the frequencies that are generated by the transmitter due to non-linearities. These frequencies are in addition to those intentionally generated, and serve to broaden

the frequency spectrum actually required for the transmission of the hybrid signal. Bruene [20] states that state-of-the-art techniques involving degenerative feedback allow third-order intermodulation products to be reduced to a level forty decibels lower than that of the desired frequencies. Use of these techniques will minimize the effects of spectrum enlargement caused by non-linearities in the transmitter.

CARRIER-FREQUENCY LEAKAGE AT THE MODULATOR

Generation of the single and double-sideband signals in the modulator portion of the hybrid-system transmitter will require suppression of the carrier frequency. The balanced modulators used to obtain this suppression are not perfect devices and do not provide absolute elimination of the carrier component. The degree of suppression is a function of circuit design, shielding, initial component balance, and the unbalancing effects caused by component aging and environment.

Appendix I contains the solution of the demodulator action when the input signal to the receiver contains a carrier-frequency component. The results of this analysis show that the carrier component is effectively ignored by the demodulator and does not influence its operation in any manner.

The power-amplifying stages of the transmitter will be influenced by the amplitude of the carrier-frequency component, as the average power content of the hybrid signal will be increased by this amount. This should not pose a significant problem since a carrier suppression of thirty decibels is easily achieved with circuits in common use.

The effects of non-linearity in either the transmitter or the receiver were shown in an earlier section for conditions of no carrier-frequency component. If the amplitude of the carrier component is

appreciable as compared with the desired signal-frequency components, the third-order intermodulation products must be re-examined.

Using the procedure established earlier in this Chapter:

$$\begin{aligned}
 (68) \quad (a) \quad & \omega_c - \omega_s \\
 (b) \quad & \omega_c + \omega_s \\
 (c) \quad & \omega_c - \omega_i \\
 (d) \quad & \omega_c
 \end{aligned}$$

The products formed by combinations of (a), (b), and (c), are shown by Equations (62) through (67). When (d) is included, the additional products are:

$$(69) \quad 2d-a = \omega_c + \omega_s$$

$$(70) \quad 2a-d = \omega_c - 2\omega_s$$

$$(71) \quad 2d-b = \omega_c - \omega_i$$

$$(72) \quad 2b-d = \omega_c + 2\omega_s$$

$$(73) \quad 2d-c = \omega_c - \omega_i$$

$$(74) \quad 2c-d = \omega_c + 2\omega_i$$

The existence of the carrier-frequency components and the effects of non-linearities in the transmitter are seen to broaden the spectrum required for transmission. At the demodulator these additional frequencies can produce interference within the intelligence passband, as shown by Equations (72) and (74).

Maximum suppression of the carrier-frequency component in the modulator is necessary to achieve minimum spectrum bandwidth requirements, minimum distortion of the intelligence information and maximum utilization of power amplifier capabilities.

The strength of the received signal will vary over wide limits due to the effects of non-uniform propagation through the transmission

medium. The basic demodulator circuitry will become overloaded if the amplitude of its input becomes too great, causing the audio-frequency intelligence output to become distorted by exceeding the linear operating ranges of the individual stages. Also, excessive amplitude may cause the narrow-bandpass filters in the synchronizing circuits to ring, generating spurious transients in the gated rectifier which will disturb the phase-locking operation.

Under fading conditions which cause the amplitude of all components of the received hybrid signal to fall below the threshold strength required for proper demodulator operation the intelligence output will disappear and the frequency of the reinserted carrier will vary.

The problems created by input signals of high amplitude can be minimized by the use of automatic-gain-control circuitry in the demodulator. This circuitry must provide rapid-attack characteristics in order that the receiver and demodulator do not overload on peaks of the received voice signal, and slow-release characteristics to maintain relatively constant gain between words and syllables. These requirements are not easily achieved when suppressed-carrier signals are involved, as the control must be derived from the demodulated audio information rather than from the carrier level, as can be done when receiving non-suppressed-carrier signals. Audio-derived control information must necessarily be integrated over a period of time so that the gain will not be varied with the instantaneous amplitude of the voice waveform. The means that were used to provide these characteristics in the laboratory model will be discussed in Chapter IV.

Drifting of the frequency of the reinserted carrier during periods when the amplitude of the synchronizing components ($\omega_c - \omega_s$) and

(0.1), if the received signal fall below the threshold value required for proper synchronizing action can be minimised by providing a long time constant in the phase-locking system. This low-amplitude condition may be encountered during periods of flat-frequency fading, where all components of the hybrid signal fade simultaneously, or during those periods of selective fading, where the amplitude of the synchronizing-frequency components fade, but the other frequencies of the hybrid signal do not fade simultaneously.

The selection of the length of the time constant in the phase-locking system must provide a compromise between that value which will correct for rapid frequency variations, and that which will minimize the drift of the reinserted-oscillator frequency during periods when the amplitude of the received synchronizing-frequency components falls below threshold.

CHAPTER IV

THE LABORATORY MODEL

In order to ascertain the practicability of the hybrid-sideband communications system, laboratory models of the basic modulator and demodulator were constructed and tested. This chapter describes the models constructed, measurements performed, and the results obtained.

MODULATOR

The modulator performs the two basic functions of generating a fixed frequency, double-sideband suppressed carrier signal for synchronizing purposes, and generating a single-sideband suppressed carrier signal to convey the intelligence information. Figure 1 shows the general format of the output required of this unit. The contents of articles by Stoner [17], ARRL [18], and Weaver [6] were studied prior to the selection of the actual circuitry which is shown in Figure 10.

For design considerations the modulator was divided into three sections:

- (1) The Carrier-Frequency Generator
- (2) The Single-Sideband Generator
- (3) The Double-Sideband Generator

CARRIER-FREQUENCY GENERATOR

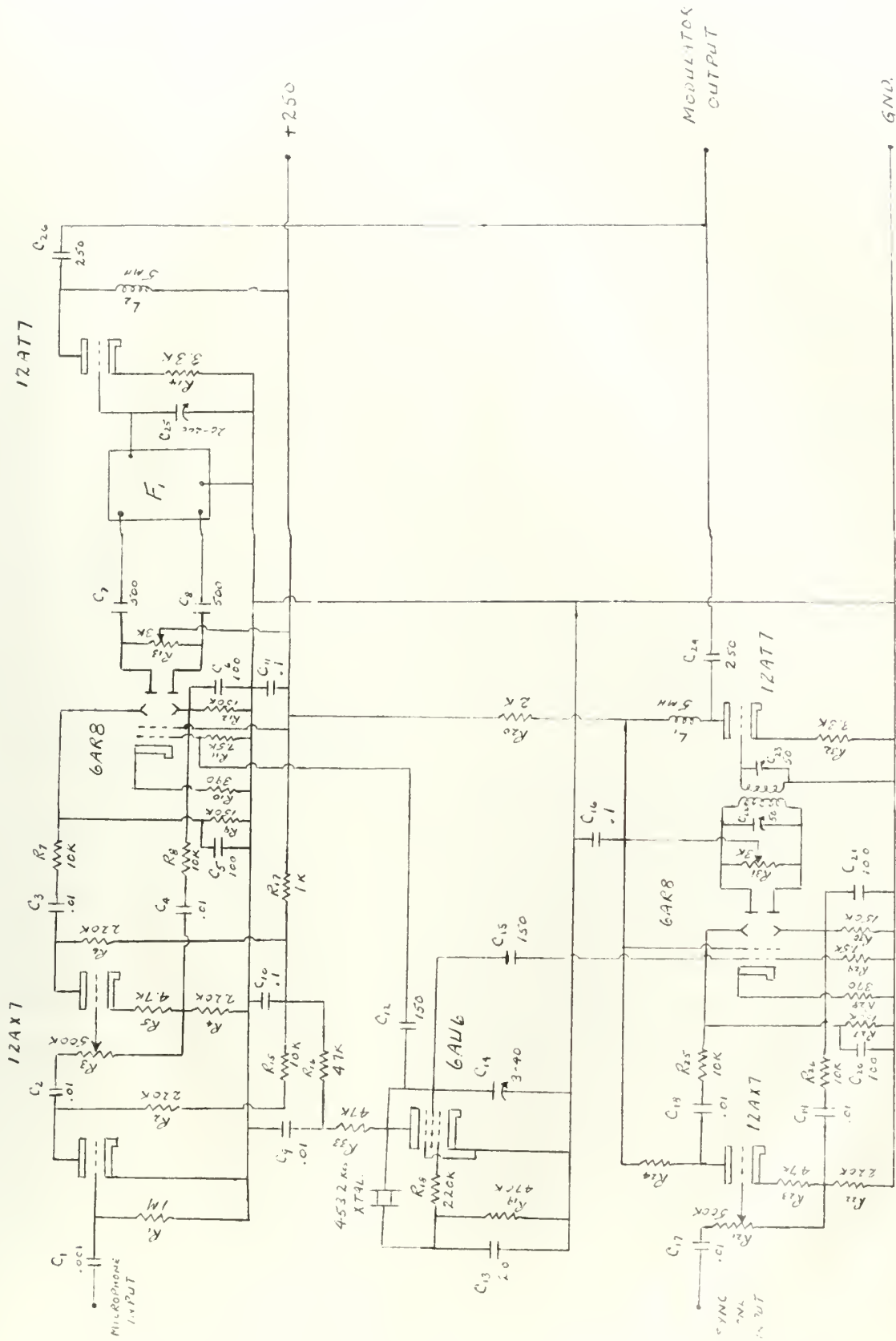
The original design of this unit was based upon the use of a series-tuned Clapp oscillator operating at a frequency of 453.2 kilocycles per second. (Selection of this particular frequency will be justified in the next section of this chapter.) High-Q inductors and silver-mica capacitors were employed in an attempt to maximize frequency stability. Every effort was made to provide rigid wiring, thermal and electrical isolation, and temperature compensation in order to further aid in

achieving a high degree of stability; however, subsequent testing of this completed model revealed that a short-term stability of only 50 cycles per second could be obtained. This was not considered to be satisfactory in view of the detailed system testing which would require stability of less than twenty cycles per second, necessitating the redesign and rebuilding of this unit.

A piezo-electric crystal with a series-resonant frequency of 453.2 kilocycles per second was obtained, and the carrier-frequency oscillator circuitry was altered to provide a crystal-controlled oscillator configuration. A series of models were constructed with provisions for varying all of the pertinent circuit parameters. As a result of measurements conducted on these models, the circuit configuration shown in Figure 10 was selected, as this provided the maximum frequency stability under conditions of varying supply potentials and ambient temperatures.

During the aforementioned measurement program it was noted that there existed a high degree of carrier-frequency radiation from the metal-encased piezo-electric crystal. This radiation was minimized in the final model by placing the crystal unit within the shielded enclosure which contained the resistor and capacitor components of the carrier-frequency generator. The 6AU6 tube, is the only component not housed within this enclosure. As a further precaution against stray coupling of the carrier frequency into other portions of the modulator, all leads which entered this enclosure were filtered with feed-through type capacitors.

A series of measurements were made, using the AN/PRM-1 Field Intensity Meter with a small coupling loop, to determine the effectiveness of the measures taken to isolate this stage. When the envelope of the tube was shielded, no radiation in excess of two microvolts per meter was



detected outside the confines of this shielded enclosure. This low level was deemed to be very satisfactory for the intended usage.

A counter-type frequency meter was used to measure frequency stability. When the high-voltage supply to the oscillator stage was maintained within plus and minus one-half percent, a maximum frequency change of only six cycles per second was observed during a four hour period. Variation of this supply potential between the limits of 150 and 340 volts caused a maximum frequency change of only eighteen cycles per second.

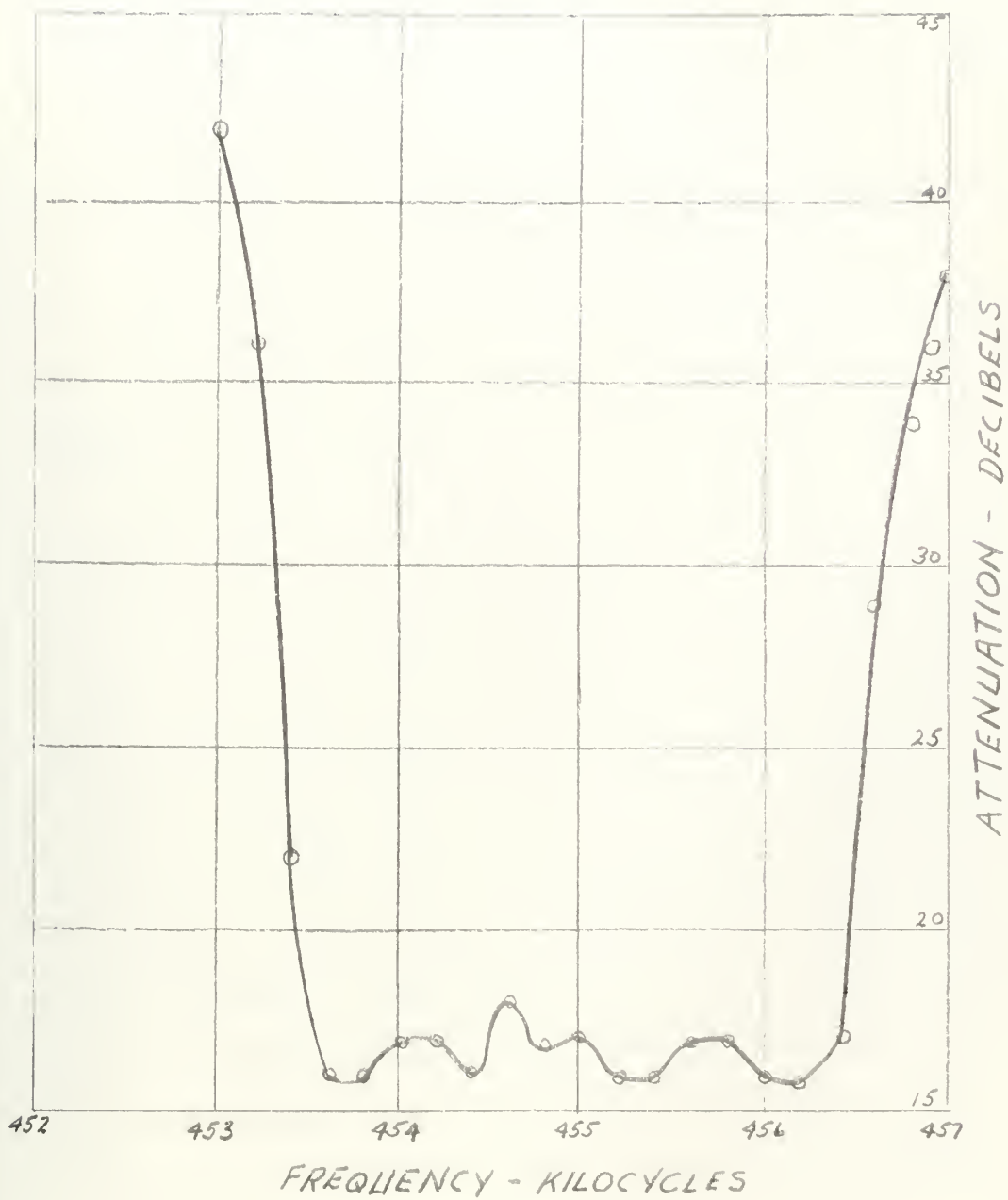
The output waveform of this oscillator was viewed on a dual-beam oscilloscope, where it was compared with a sine wave obtained from a high quality audio-frequency oscillator. When the two waveforms were superimposed no differences were noted.

In view of the satisfactory results obtained during the testing of this unit, no further circuit modifications were made.

THE SINGLE-SIDEBAND GENERATOR

The design of this portion of the modulator was determined by the ready availability of a 455 kilocycle per second Collins mechanical filter. The results of laboratory measurements performed upon this filter are shown in Figure 11. Following the manufacturers' recommendations the frequency of the carrier-frequency oscillator was selected to coincide with the minus twenty decibel attenuation point shown in this figure. Availability of a 453.2 kilocycles per second crystal for the Carrier Frequency Generator dictated that the single-sideband output of the modulator appear as the upper sideband with reference to the carrier frequency.

The circuitry used to obtain the single-sideband output consists



PASSBAND CHARACTERISTICS
MECHANICAL FILTER

FIGURE 11

of the following:

- (A) An audio-frequency amplifier to provide sufficient amplification for use with a high impedance source such as a crystal microphone.
- (B) A balanced modulator to obtain a double-sideband suppressed carrier signal.
- (C) A filter to suppress the lower sideband and the carrier frequency.

The audio amplifying stage employs resistance-capacitance coupling and uses one section of a 12AX7 tube. Gain of this stage is 75. Input impedance is approximately 400,000 ohms.

Many different types of balanced modulators are described in the literature. The ring modulator configuration using solid-state diodes is widely used for single-sideband modulator applications, however, this circuit requires a balanced oscillator input of several volts. Also, the impedance presented by the ring modulator to the carrier-frequency generator and to the audio source varies over the cycle, requiring low impedance balanced outputs from these two sources. In order to minimize the circuitry problems posed by these requirements, the balanced-modulator configuration selected was one employing a gated sheet-beam deflection tube, as described by Stoner [17]. This circuit has the advantage of requiring only one volt of carrier level from an unbalanced, high-impedance source; however, a balanced audio-frequency input on the order of fifteen volts is needed. The audio frequency source requirement is easily achieved by the use of a paraphase inverter which utilizes one section of a 12AX7 tube. The carrier-frequency source is capacitively coupled to the 6AR8 gated sheet-beam tube, and

its relatively low level simplifies the problems associated with isolating this source from the remainder of the modulator circuitry.

The 6AR8 tube contains a cathode, control-grid, and screen grid which form an electron gun to generate, control, and accelerate a beam of electrons. There are two anodes, and a pair of deflecting plates associated with those anodes. The total current to the two anodes is determined by the potentials applied to the cathode and the two grids, division of this current between the two anodes being controlled by the potential difference between the two deflecting plates. To achieve the switching action required for balanced modulator operation the carrier frequency source is coupled to the control grid where it varies the intensity of the electron stream, and the push-pull audio-frequency source is coupled to the two deflecting electrodes to switch the electron flow between the two anodes at an audio rate. The anode circuitry external to the tube consists of a balanced, center-tapped load tuned to the carrier frequency, which acts to provide cancellation of the carrier frequency, since this was effectively applied in parallel to the two anode electron paths. The frequency components present at the load consist of the two symmetrical sidebands and the suppressed carrier. The audio-frequency component is very greatly attenuated due to the low impedance presented to these frequencies by the load, which is tuned to the carrier frequency.

A model of this circuit was constructed and resulting measurements revealed that a carrier suppression in the order of twenty-five decibels could be achieved. Additional testing indicated that the maximum degree of possible suppression varied considerably when several different 6AR8 tubes were tried. Careful tube selection was required to achieve sup-

precision in order of 100000 decibels.

The type 7360 tube which was recently announced by the Radio Corporation of America is a redesign of the type 6AR5 pentode sheet-beam tube. This newer tube is held to stringent manufacturing tolerances, and is electrically superior to the 6AR5. Three samples of the 7360 were obtained and tested in a laboratory circuit. Carrier suppression of fifty decibels was achieved, and this figure was maintained when the three tubes were interchanged. Unfortunately, the modulator construction had been completed prior to the availability of this superior tube, and the fact that the base connections differed from those of the 6AR5 precluded its use in the modulator.

The mechanical filter which has the passband characteristics shown in Figure 11 is used as the tuned load for the balanced modulator. Collins [19] gives a physical description of the operation of this device. External resonating capacitors are included in the modulator circuitry to resonate the inductive input and output impedances of the filter. When properly terminated, the passband insertion loss for the particular filter used was sixteen decibels, however, this loss was considered to be justified in view of the excellent filtering characteristics obtained. Improved filters with lower insertion loss are obtainable, but were not available for this construction.

The output of the filter is fed to the grid of an amplifier stage which employs one section of a 12AT7 tube. This stage is used to provide isolation between the outputs of the single and double-sideband generators as these two outputs are parallel-connected in the anode circuit of this stage.

THE DOUBLE SIDEBAND GENERATOR

The balanced modulator circuitry used in this generator is fundamentally identical to that employed in the Single-Sideband Generator. The only difference is the use of a tuned transformer in the anode circuit in place of the mechanical filter which was used in the Single-Sideband Generator. The paraphase amplifier stage used to obtain the push-pull high impedance audio drive for the balanced modulator is identical to that previously described. As this generator is required to produce a double-sideband signal that is modulated by a fixed, single frequency, no audio amplifier circuitry preceeds the paraphase amplifier. A laboratory-type audio frequency oscillator tuned to the synchronizing frequency is connected directly to the input of the paraphase stage. The output amplitude of this oscillator is adjusted to provide an eighteen volt signal at the deflecting anodes of the gated sheet beam tube.

The secondary winding of the tuned transformer used in the anode circuit of the balanced modulator is coupled to the grid of a 12AT7 tube used as an isolating amplifier. The anode circuitry of this tube is capacitively coupled to the output of the modulator, in parallel with the capacitively coupled output of the isolating amplifier stage of the Single-Sideband Generator.

The original laboratory model of the modulator did not include the two isolating amplifier stages, the outputs of the mechanical filter and the tuned transformer being parallel connected. During the testing of this model it was observed that interaction existed between the Single and Double-Sideband Generators. Insertion of the isolating stages was found to completely solve this problem.

The output of the modulator is fed to a linear mixer type of frequency translator in order to relocate the hybrid signal from the intermediate frequency range to the desired radio frequency. Since the mixing process produces additional frequency components, highly selective circuits must be used to suppress the undesired components. In a practical transmitter several translators might be required in order to achieve the desired suppression of these components. The laboratory model employed only one stage of translation, and the radio frequencies used for testing were confined to the lower portion of the high-frequency bands.

Laboratory measurements were performed on the completed modulator using the Panoramic Radio Company Model SSB-3 spectrum analyzer. Entirely satisfactory operation was noted, as is indicated below:

- (1) Intermodulation distortion products were found to be at least thirty-eight decibels below the level of the desired tone frequencies.
- (2) The undesired sideband output of the Single-Sideband Generator was found to be at least forty-one decibels below the level of the desired sideband.
- (3) The carrier frequency output of the Double-Sideband Generator was suppressed to a level of twenty decibels lower than that of the double-sideband components.
- (4) The carrier-frequency output of the Single Sideband Generator was suppressed to a level of forty decibels less than that of the desired sideband.

As a result of these satisfactory measurements the laboratory model of the modulator was considered completed.

THE DEMODULATOR

A block diagram of the demodulator is shown in Figure 2. The circuit given by Webb [5], which is suitable for the reception of single or double-sideband signals was used as the basis for the laboratory model of the demodulator which was constructed for use with the hybrid-sideband communications system. A schematic diagram of the laboratory demodulator is shown in Figure 3.

The product detectors, V-1 and V-2, are identical to those given by Webb [5]. The incoming signal is applied to the grids of V-1A and V-2A which are used as cathode followers, whose outputs are directly coupled to the cathodes of V-1B and V-2B. The reinjected oscillator voltages are applied to the grids of V-1B and V-2B. Since the electron stream of V-1B and V-2B are modulated by the signals applied to both the cathodes and the grids, the anode current is a function of the product of these two modulating signals. This operation may be shown as:

$$(75) \quad i_p = (a + b e_1 + c e_2 + d e_1 e_2)$$

where: i_p = instantaneous anode current

e_1 = instantaneous cathode potential

e_2 = instantaneous grid potential

a, b, c, d = constants which are functions of tube parameters

Expanding:

$$(76) \quad i_p = ac + a d e_2 + b c e_1 + b d e_1 e_2$$

Inspection of this equation reveals that the output of the product detector will be comprised of:

- (1) A direct current term, ac .

(2) Components of the two input signals, as represented by ade_2 and bce_1 .

(3) A term, bde_1e_2 , which represents the product of the instantaneous values of the two input signals.

As shown in Chapter II, the product term is the only portion of the output that is desired for this application. The direct current term is blocked by the output coupling capacitor, and the components of the input frequencies are suppressed by the low-pass filters, F_1 and F_2 , which follow the product detectors.

In the laboratory model the low-pass filtering is accomplished with the simple resistor-capacitor networks comprised of C-2, R-4, C-3, R-5, and C-12, R-29, C-13, R-30. These are low pass networks whose attenuation is small for frequencies up to 10,000 cycles per second, but becomes approximately 60 decibels in the vicinity of the frequency of the reinserted-oscillator signal. The outputs of these filters are fed to both the signal path and to the phase-locking loop after passing through resistance-coupled amplifier stages V-3A in the I channel and V-3B in the Q channel. These stages are included to provide additional amplification of the product detector outputs and are directly coupled to the phase-shifting stages V-4A and V-4B in order to eliminate additional phase shifts at the lower audio frequencies.

The phase-locking loop take-off is fed through isolating amplifiers comprised of V-6A and V-6B, which are resistance coupled to the bandpass filters F-3 and F-4, tuned to the audio synchronizing frequency. Matched filters tuned to 250 cycles per second were available, so that this frequency was selected for synchronizing purposes. Fol-

lowing these filters are V-7A and V-7B which are used as paraphase amplifiers to obtain balanced inputs to the gated rectifier circuitry. Output of the gated rectifier is coupled to the reactance control tube V-8B, through the lag network which is comprised of R-49, R-50, and C-31. The values of these components were determined from Equations (56) and (57) to provide a lock range of 300 cycles per second and a capture range of 200 cycles per second.

The anode of V-8B is coupled to the grid-tank circuit of the reinjection oscillator to permit the frequency of this oscillator to be varied in accordance with the magnitude of the voltage output of the gated rectifier. The oscillator circuit employs the tuned-grid configuration. Output from this stage is taken from the cathode circuit to obtain a low source impedance and an amplitude of approximately two volts. V-9 is used as a cathode follower to isolate the frequency-determining elements of the oscillator from impedance variations during alignment of subsequent portions of the circuitry. Following this stage is the resistor-capacitor network which is used to obtain the required ninety-degree phase difference between the reinjected-oscillator signals which are applied to the two product detectors. When the resistors R-41 and R-42 are identical and are equal to the identical reactances of the two capacitors C-21 and C-23, the two outputs taken from the junctions of R-41-C-21 and R-42-C-23 are equal in magnitude and ninety degrees different in phase relationship. A variable capacitor was used for C-23 to allow adjustment to compensate for stray circuit capacitances.

The intelligence signal path take-off points at the plate circuits of V-3A and V-3B are coupled to the magnitude-proportioning phase-

splitting stages V-4A and V-4B which use a 12AT7 tube to obtain the required inputs for the Millen phase-shifting networks. The manufacturer specifies that the two inputs to each of the I and Q networks have 180-degrees phase difference, and furthermore, that these two voltages be in a seven-to-two proportion. These requirements were met by the use of a paraphase-amplifier configuration with the ratio of the plate and cathode resistances being seven-to-two. Proper operation of the phase-shifting networks is very dependent upon this ratio, dictating the requirement for one-percent tolerance components in this stage.

Outputs from the phase-shifting networks are fed to a pair of paraphase amplifiers having identical plate and cathode resistances. The cathode of V-5A is fed directly to one end of the adder-subtractor network comprised of resistors R-15, R-16, and R-40. Output of the Q channel paraphase inverter, V-5B, is taken from either the plate or cathode of this tube, depending upon the selected setting of switch S-1. When S-1 is connected to the cathode of V-5B, the polarities of the output contributions from both the I and Q channels are in-phase, causing the signal voltage developed across the load resistance R-79 to be proportional to the mathematical sum of the I and Q channel outputs. As shown in Chapter II this will cause the lower sideband of the incoming signal to be suppressed. When S-1 is connected to the plate circuit of amplifier V-5B, the Q channel output contribution is phase-shifted by 180 degrees from that of the I channel, causing the voltage across the load resistance R-79 to be proportional to the mathematical difference of the I and Q channel outputs. When connected in this manner the upper sideband of the incoming signal will be suppressed.

The selection of the setting of switch S-1 is determined by the type of hybrid signal emitted by the modulator portion of the transmitting equipment. If the modulator is designed to position the desired intelligence information in the upper sideband, S-1 must be connected to the cathode of V-5B. This will allow reception of the upper sideband while attenuating noise and interfering signals which may be present in that portion of the frequency spectrum which forms the lower sideband.

Following the adder/subtractor network are three stages of audio-frequency amplification and band-pass filter. The amplifier consists of one section of a 12AX7 tube used as a preamplifier which is resistance coupled to another stage using the same type tube. This second stage, V-108, is used to provide additional amplification and to match the input impedance of the 300-3000 cycle per second bandpass filter that is capacitively coupled to the output of this stage. This filter serves to suppress the 250 cycles per second synchronizing-tone frequency in order to prevent this component from appearing with the intelligence information. Following this filter is a power amplifier stage, V-11, which is transformer coupled to the loudspeaker output.

The automatic-gain-control circuit used in the laboratory model of the hybrid-sideband demodulator achieves both rapid-attack and slow-release characteristics by using a silicon diode connected in shunt with the filter resistance of the automatic-gain-control rectifier. This circuitry is shown in Figure 3.

When a high-amplitude signal is received, the output of the rectifier, V-6A, rapidly charges the capacitor C-43, as the filter resistor,

R-72, is bypassed by the forward-biased silicon diode, D-5. As the amplitude of the received signal varies below the voltage to which the capacitor is charged, the output of the rectifier will be lower than the capacitor voltage, causing the silicon diode to be reverse-biased. The discharge time of this capacitor is many times longer than the charge time, as the discharging resistance is greatly increased when the shunt-connected silicon diode is reverse-biased.

In practice the values of R-72, R-73, and C-43 will depend upon the desired attack and release time constants, and upon the values of the resistance and capacitance used in the automatic-gain-control circuitry of the radio-frequency receiver which precedes the demodulator. The writers' experience has shown that an attack time of ten milliseconds and a release time of one second will provide satisfactory gain-control information for the reception of speech information.

LABORATORY EXPERIMENTS WITH THE DEMODULATOR

The laboratory model of the hybrid sideband system demodulator was assembled and the following parameters determined by measurement:

- (1) Lock range
- (2) Capture range
- (3) Suppression of undesired sideband
- (4) Ratio of input levels required for synchronizing and intelligence demodulation.

The measurement of lock and capture ranges was complicated by the non-availability of signal generators which are capable of providing a signal in the intermediate or radio frequency range and can be accurately varied about the center frequency in increments of less than fifty cycles per second. An attempt was made to utilize laboratory

type signal generators in conjunction with frequency counters, however, the inherent instability of these generators precluded accurate measurements. This problem was overcome by the use of a frequency synthesizer capable of providing frequencies from zero to 100,000 cycles per second in one cycle per second increments. A balanced mixer was constructed to translate the output frequency of this instrument to the 455 kilocycles per second operating frequency of the demodulator. The synthesizer employed regenerative frequency dividers, and one similar divider unit was constructed to permit a highly stable, one megacycle per second reference frequency source to provide a four hundred kilocycle per second signal for injection to the balanced mixer. The synthesizer was adjusted to furnish a nominal 55 kilocycles per second output frequency which was mixed with the four hundred kilocycles per second reference to obtain the desired output of 455 kilocycles per second. This output was connected to replace the Carrier-Frequency Generator in the modulator. The synthesizer frequency was then varied to determine the lock and capture frequency ranges of the demodulator. It was found that once the reinserted-carrier frequency was locked by inserting a 455 kilocycle per second signal the phase-locking loop would not unlock until the input frequency reached the extremes of 454.795 and 455.175 kilocycles per second, indicating that a lock range of 380 cycles per second was achieved. The unsymmetrical deviations above and below the center frequency is attributed to imperfect balance of the phase detector and the non-linear transfer function of the reactance tube and oscillator.

The capture range was determined by displacing the synthesized frequency from 455 kilocycles per second and slowly varying this fre-

quency toward 455 kilocycles per second until demodulator locking was achieved, as evidenced by the disappearance of a heterodyne note in the intelligence output. It was found that a capture could be achieved at the frequencies of 454.890 and 455.120 kilocycles per second, indicating a capture range of 230 cycles per second.

Suppression of the undesired sideband was measured by the following method:

- (1) The phase-locking feature was disabled by positioning the AFC ON-OFF switch, S-2, in the OFF position.
- (2) The frequency of the reinserted carrier was set to 453.2 kilocycles per second by adjusting C-27.
- (3) An A.C. voltmeter was connected to the grid of the audio-frequency power amplifier tube, V-11.
- (4) The output of a radio-frequency signal generator was connected to the input of the demodulator.
- (5) The frequency of the signal generator was set to 455.0 kilocycles per second to provide an 1800 cycle per second output from the demodulator.
- (6) The reading of the voltmeter was observed and recorded.
- (7) The signal generator was adjusted to furnish an output frequency of 451.2 kilocycles per second.
- (8) The reading of the voltmeter was observed and recorded.
- (9) The suppression of the undesired sideband was obtained from the difference of the two voltmeter readings. This value was found to be 28 decibels.

The ratio of input levels required for synchronizing and for reproduction of the intelligence information was determined by the fol-

lowing procedure:

- (1) An A.C. voltmeter was connected to the output of the band-pass filter, F-4, which is in the Q channel.
- (2) The output from the double-sideband generator was connected to the input of the demodulator through a variable attenuator.
- (3) The input level to the demodulator was gradually increased by reducing the attenuator setting, until the voltmeter reading was observed to increase.
- (4) The attenuation was further increased until the voltmeter reading decreased to a null value. (This null in the output of the Q channel to the gated rectifier indicates that phase lock has been achieved, as can be seen from Equation (46).)
- (5) The output voltage of the attenuator was measured and found to be .03 volts.
- (6) The output of the single-sideband generator portion of the modulator was connected to the input of the demodulator. This generator was modulated with a frequency of 1,000 cycles per second.
- (7) The output level of the single-sideband generator was adjusted until the 1,000 cycle per second tone was clearly audible from the loudspeaker connected to the demodulator output.
- (8) The output voltage of this generator was measured and found to be 0.93 volts.
- (9) The ratio of power required for synchronizing to that required for audible intelligence output was determined as:

CHAPTER V

CONCLUSIONS

The results of the system tests which were described in the previous chapter substantiate the theoretical development given in Chapter II. Many of the significant problems which might arise in practical implementation of the hybrid sideband system have been investigated, and are described in Chapter III.

The proposed model of the receiving system which is described in this paper was based upon the use of phasing techniques for elimination of the undesired sideband. This approach was taken because the phase-shifted reinjection oscillator and quadrature-operated product detectors that are required for demodulation of single-sideband signals by the phasing method were also required for the basic phase-locking circuitry. Although not verified experimentally, it should be feasible to use filtering techniques for elimination of the undesired sideband, particularly if the additional component cost is not of prime importance.

Use of the hybrid sideband system in lieu of the single-sideband system will enable frequency stability requirements to be appreciably relaxed. This will reduce the procurement and maintenance costs of communication systems, and provide automatic, rapid correction for frequency shifts caused by Doppler Effect when communicating with high performance aircraft.

The bandwidth requirements of the hybrid sideband system are only 550 cycles per second greater than those of the single-sideband system when using voice transmission of frequencies between 300 and 3000 cycles per second. This small increase of bandwidth appears to be well justified in view of the advantages described in the previous paragraph.

The hybrid sideband signal that is transmitted is compatible with existing single sideband receiving equipments. In some instances it may be necessary to install a filter in existing receivers to suppress the synchronizing tone frequency, however, this could easily be inserted in the output leads and located externally. The majority of receivers should not require this modification, as their bandpass characteristics will provide sufficient suppression of the synchronizing tone.

The receiver-demodulator as employed with the hybrid sideband system is completely compatible with the other types of communications systems in common use, such as: single sideband, continuous wave, and frequency shift. Reception of double-sideband suppressed carrier signals and ordinary double-sideband amplitude modulated signals, which require that the reinsertion oscillator be phase locked with the transmitter frequency can be easily accomplished by disabling the two tuned-bandpass filters in the demodulator synchronizing circuit.

The transmission of a carrier-frequency signal whose amplitude is reduced by about twenty decibels from that of the intelligence-bearing single sideband has been used in conjunction with exhalted-carrier receiving techniques to provide a reinserted carrier of the proper frequency. A filter with extremely-narrow bandpass is employed at the receiver to separate the carrier frequency from the modulation frequencies. This carrier-frequency signal is then amplified and applied to a product detector.

Although it was not verified experimentally, the hybrid-sideband system should provide better operation than this reduced-carrier system under conditions of poor signal-to-noise ratio, as the narrow-bandpass filters are prone to ring, causing spurious frequencies to be reinserted

at the product detector. These spurious frequencies will generate distortion products which will appear in the output of the receiver.

Although this paper has treated only the use of voice communications, the ability of the hybrid-sideband system to provide a phase-locked re-inserted carrier can be employed advantageously for binary data communications.

The automatic-gain-control feature of the hybrid-system demodulator could be achieved by using either the intelligence information or the synchronizing signal as the basis for the derivation of the control potential. Use of the former source was selected as it provides a control potential which varies directly with the level of the desired output of the demodulator. Derivation of the control potential from the double-sideband synchronizing signal will not provide the required gain control function under conditions of selective fading, as the frequency used for the synchronizing information is not contained within the passband of the intelligence information. Under conditions of selective fading the received level of the synchronizing frequency can vary independently of the frequencies conveying the intelligence information, causing the control potential to vary the gain of the receiver in a manner that will not necessarily maintain the level of the desired audio-frequency output.

It was shown in Chapter II that the proper operation of the demodulator is dependent upon amplitude and phase balance between the I and Q channel circuitry. Much work was required to achieve this symmetry while adjusting the laboratory model, and it is anticipated that these requirements may complicate the production and maintenance of this equipment. The laboratory model was found to operate satisfactorily

during a continuous three-week period after the symmetry requirements had been achieved, however, subsequent replacement of one of the product-detector tubes necessitated realignment of the phase-locking circuitry.

It is recommended that any future work on the hybrid-sideband communications system include a study of the effects of selective fading upon the frequency of the reinserted carrier; and that serious consideration be given to the use of filtering techniques for suppression of the undesired sideband in order to reduce the number of stages requiring critical phase and amplitude balance.

BIBLIOGRAPHY

1. Norgaard, D. E., "The Phase Shift Method of Single-Sideband Reception," Proceedings of the Institute of Radio Engineers, 44: 1735, December, 1956.
2. Dome, R. B., "Wide-band Phase Shift Networks," Electronics, 19: 112-115; December, 1946.
3. Darlington, S., "Realization of a Constant Phase Difference," Bell System Technical Journal, 24: 94-104; January, 1950.
4. Costas, J. P., "Synchronous Communications," Proceedings of the Institute of Radio Engineers, 44: 1713-1718; December, 1956.
5. Webb, J. K., "A Synchronous Detection Adapter for Communications Receivers," CQ Magazine: 34-37; June, 1957.
6. Weaver, D. K., "Quadrature Signal Functions and Applications," Study Report - Montana State College: 89-91; December, 1958.
7. Nupp, W. D., "Effects of Selective Fading on AM Signals," Thesis, University of Pennsylvania: 39-41; June, 1957.
8. McAleer, H. T., "A New Look at the Phase-Locked Oscillator," Proceedings of the Institute of Radio Engineers, 47: 1137-1143; June, 1959.
9. Wood, R. H. and Whyland, W. P., "A Synchronous Communications Receiver for the Military UHF Band," IRE Transactions on Communications Systems, CS-7: 129-133; June, 1959.
10. Craiglow, R. L. and Martin, E. L., "Frequency Control Techniques for Single Sideband," Proceedings of the Institute of Radio Engineers, 44: 1697-1702; December, 1956.
11. Gruen, W. J., "Theory of A.F.C. Synchronization," Proceedings of the Institute of Radio Engineers, 41: 1043-1049; August, 1953.
12. Laden, H. N., "Wideband Phase Shift Networks for Single Sideband Transmitters," Thesis- U. S. Naval Postgraduate School; 1949.
13. Norgaard, D. E., "The Phase-Shift Method of Single-Sideband Signal Generation," Proceedings of the Institute of Radio Engineers, 44: 1718-1735; December, 1956.
14. Villard, O. G., "Cascade Connection of 90-Degree Phase Shift Networks," Proceedings of the Institute of Radio Engineers, 40: 344-337; March, 1952.
15. Luck, D. G. C., "Properties of Some Wide-Band Phase-Splitting Networks," Proceedings of the Institute of Radio Engineers, 37:

147-151; February, 1949.

16. Icenbice, P. J. and Felhauer, H. E., "Linearity Testing Techniques for Sideband Equipment," Proceedings of the Institute of Radio Engineers, 44: 1775-1782; December, 1956.
17. Stoner, D. S., New Sideband Handbook, Cowan Publishing Corporation, 1958.
18. ARRL, Single Sideband for the Radio Amateur, American Radio Relay League, 1954.
19. Collins, "SSB Techniques," published by Collins Radio Company, 1959.
20. Bruene, W. B., "Distortion Reducing Means for Single-Sideband Transmitters," Proceedings of the Institute of Radio Engineers, 44: 1760-1765; December, 1956.
21. Honey, J. F., "The Problems of Transition to Single-Sideband Techniques in Aeronautical Communications" Proceedings of the Institute of Radio Engineers, 44: 1803-1810; December, 1956.

APPENDIX I

OPERATION OF HYBRID SYSTEM DEMODULATOR WHEN RECEIVED

SIGNAL CONTAINS A CARRIER FREQUENCY COMPONENT

The received signal may be represented as:

$$e_s = A \cos(\omega_c t + \phi) + A \cos(\omega_c t + \phi + \pi) = A \cos(\omega_c t + \phi) - A \cos(\omega_c t + \phi + \pi)$$

The I channel product detector receives both e_s and the oscillator injection, $E \cos \omega_c t$. Output of this detector is:

$$\begin{aligned} e_{oi} &= e_s * E \cos \omega_c t \\ &= \frac{AE}{2} [\cos(2\omega_c - \omega_s)t + \cos(2\omega_c + \omega_s)t + \cos(2\omega_c - \omega_s)t + \cos(2\omega_c + \omega_s)t] \\ &\quad + \frac{CE}{2} [\cos 2\omega_c t] + \frac{DE}{2} [\cos(2\omega_c + \omega_s)t + \cos(2\omega_c - \omega_s)t] \end{aligned}$$

The Q channel product detector receives both e_s and the phase-shifted oscillator injection, $E \sin \omega_c t$. Output of this detector is:

$$\begin{aligned} e_{oq} &= e_s * E \sin \omega_c t \\ &= \frac{AE}{2} [\sin(2\omega_c - \omega_s)t + \sin(2\omega_c + \omega_s)t] \\ &\quad + \frac{CE}{2} \sin 2\omega_c t + \frac{DE}{2} [\sin(2\omega_c + \omega_s)t - \sin(2\omega_c - \omega_s)t] \end{aligned}$$

After passing through the low-pass filters which succeed the product detectors, the outputs become:

$$e_{r1} = AE \cos \omega_s t + \frac{DE}{2} \cos \omega_s t$$

$$e_{r2} = -\frac{DE}{2} \sin \omega_s t$$

These two signals are then treated by the β and $\beta + 90^\circ$ phase shifting networks. These networks serve to advance the phase of the Q channel signal by β degrees, and that of the I channel signal by $\beta + 90^\circ$. The outputs of these networks are:

$$e_{\alpha_i} = AE \cos(\omega_s t + \beta + 90^\circ) + \frac{DE}{2} \cos(\omega_s t + \beta + 90^\circ)$$

$$e_{\beta_i} = -\frac{DE}{2} \sin(\omega_s t + \beta)$$

and since: $\cos(x + 90^\circ) = -\sin x$, these may be represented as:

$$e_{\alpha_i} = -AE \sin(\omega_s t + \beta) - \frac{DE}{2} \sin(\omega_s t + \beta)$$

$$e_{\beta_i} = -\frac{DE}{2} \sin(\omega_s t + \beta)$$

These two signals are applied to the electrical addition network. Output of this network is:

$$e_{\text{out}} = e_{\alpha_i} + e_{\beta_i} = -DE \sin(\omega_s t + \beta) - AE \sin(\omega_s t + \beta)$$

The synchronizing frequency, ω_s , is then filtered to obtain the intelligence output:

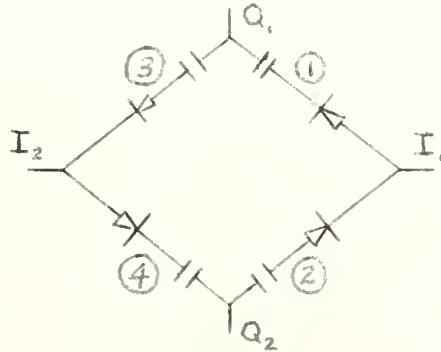
$$e_{\text{int}} = -DE \sin(\omega_s t + \beta)$$

This output, which contains only the desired information, is seen to be identical in form to that obtained when the received signal did not contain the carrier frequency component. The operations performed by the hybrid-sideband system demodulator are therefore not modified by the presence of the carrier frequency.

APPENDIX II

QUALITATIVE ANALYSIS OF THE GATED RECTIFIER

A simplified schematic diagram of the gated rectifier is shown below.



The columns headed I_1 and Q_1 are the simultaneous polarity at these locations on the sketch shown above. The columns headed 1 to 4 are the type of charge accumulation at the designated points in the circuit. The large plus or minus sign is the contribution of the I channel and the small plus or minus sign is the contribution of the Q channel.

Condition	I_1	Q_1	1	2	3	4
1	+	+	+ -		- -	
2	-	-		- -		+ -
3	+	-	+ +		- +	
4	-	+		- +		+ +
5	+		+		-	
6	-			-		+
7		+			-	+
8		-	+	-		

To obtain the polarity of the D.C. output from the gated rectifier,

the charge accumulations shown in the table above for the applicable portions of the modulation frequency cycle are added. In this process a large sign will cancel a large sign of opposite polarity, and a small sign will cancel a small sign of opposite polarity. The results of this process are shown below.

Signal	Conditions to be Added	Output Voltage of Gated Rectifier
I signal only	5 & 6	Zero
I and Q signals in phase	1 & 2	Negative
I and Q signals in anti-phase	3 & 4	Positive
I and Q signals in quadrature	1, 2, 3 & 4	Zero

Equations (45) and (46) show that the I and Q channel inputs to the gated rectifier are in quadrature when the reinserted carrier is phase-locked to the incoming carrier signal. From the above table it can be seen that this condition will produce no output from the gated rectifier, causing the reinsertion oscillator to be in a quiescent condition when phase lock is achieved.

*The contents of this appendix were taken from Nupp [7].

thesF253

A hybrid-sideband communications system.



3 2768 002 06510 4
DUDLEY KNOX LIBRARY